Journal of Ceramic Processing Research. Vol. 20, No. 4, pp. 372~378 (2019)
(Received 15 February 2019, Received in revised form 11 July 2019, Accepted 2 August 2019)

J O U R N A L O F
Ceramic Processing Research

Effect of organic solvents on zinc oxide chemical and structural properties

F.K. Konan[a,b,*], B. Hartiti[b] and B. Aka[a]
[a]*Laboratoire d'Energie Solaire et de Nanotechnologie (LESN) - IREN (Institut de Recherches sur les Energies Nouvelles), Université Nangui Abrogoua, 02 BP 801 Abidjan, Côte d'Ivoire*
[b]*ERDyS Laboratory, GMEEMDD Group, FSTM, Hassan II Casablanca University, B.P 146, Mohammedia, Morocco*

Sol-gel method is a high yield, low cost, simple technique, and robust technology that we frequently use in our laboratory. Solvents are crucial components in specialty chemical processes, and have a significant influence on the properties of thin film materials. In this paper, a series of three spin-coated zinc oxide thin films were prepared and characterized to compare the effect of different solvents such as 2-methoxyethanol, ethanol and isopropyl alcohol (IPA) on the morphological, structural and chemical properties of coated films. To this purpose, X-ray diffraction (XRD), scanning electron microscopy (SEM) and energy dispersive x-ray spectroscopy (EDS) techniques were used. According to the results of XRD data, the presence of crystallography plane (002) wurtzite phase was revealed in all the synthesized films. The crystallite average sizes, estimated by means of Scherer formula, ranged between 28 and 43 nm as function of the nature of solvents. SEM analysis indicated that the samples exhibited dense particle morphology with grains well-ordered and EDS spectra showed Zn and O elements. The crystal qualities, grain size, diameter, d-spacing and texture coefficient of the as-grown films were affected by the type of solvent used in the ZnO layer preparation. These results suggest that it is possible to vary the chemical and structural properties of coated zinc oxide thin films by controlling the organic solvents. As 2-methoxyethanol, ethanol and IPA were used to prepare the ZnO films, highly (002)-oriented ZnO thin films were formed with 2-methoxyethanol.

Key words: ZnO; sol-gel; solvents; crystallography plane (002).

Introduction

The fields of thin film synthesis, characterization, and applications in materials science have become an identifiable unified discipline of scientific endeavor [1, 2]. Deposition and investigation of oxide materials (Al_2O_3, ZnO, TiO_2, ZrO_2, etc.) have attracted an emphasized interest in recent years due to new areas of research in solid state physics and chemistry and the large number of various advanced engineering applications [3, 4]. Among these materials, zinc oxide is one of widely studied oxide materials thanks to its properties including high chemical and thermal stability [5], low cost and non-toxicity [6], wide direct band gap of 3.37 eV [7], large exciton binding energy (~60 meV) [8], etc. Some of zinc oxide distinctive applications are blue and ultraviolet (UV) light-emitting diodes [9], hydrogen storage [10], Varistors [11], solar cells [12], gas sensors [13], and photocatalyst [14].

Currently, ZnO nanostructures are synthesized by a variety of methods, such as the low pressure chemical vapor deposition (LPCVD) [15], solvothermal method [16], ultrasonication technique [17], thermal evaporation [18], pulsed laser deposition (PLD) [19], metal organic chemical vapor deposition (MOCVD) [20], molecular beam epitaxy [21], sol-gel method [22, 23], etc. Many of these methods required specialized equipment and high consumption of materials and energy, consequently increasing production cost [15, 19-21]. Therefore, at the moment, the wet chemical spin-coating technique is the most common and promising chemical route which has been widely used for thin films deposition in particular zinc oxide. This technique, allows to obtain films at simple and low cost equipment with good properties [22, 23]. Although the sol-gel process has been known for almost a century and some of the most important aspects have been clarified, its synthesis still attracts much interest for preparation of layers due to possibility of final products to be easily controlled while varying the process conditions [22, 23].

The chemical sol-gel route has also been widely employed to synthesize semiconductor materials and enabled the control of morphology, phase, and size by setting appropriate conditions such as temperature, solvents, stirring time, and doping concentration [23-28], etc.

Some studies used different solvents sources and obtained a variety of zinc oxide microstructures. J. Wang et al. [24] used an ethanol solution mixed with zinc acetate dehydrate and monoethanolamine and the results revealed ZnO with (100), (002) and (101) planes direction. The experimental results of P. Sagar et

*Corresponding author:
Tel : +22549949434
Fax: +22502737343
E-mail: kfransisco@gmail.com

al. [25] using methanol solvent showed (002) orientation. Researchers [26, 27] studied the effect of solvents on structural and optical behaviour of ZnO thin films and reported the same c-axis orientation. Investigations conducted by K.L. Foo et al. [28] using different solvents showed that the synthetized ZnO films are polycrystalline with preferred orientation along the (002) direction, whereas the isopropyl alcohol derived films have a preferred orientation on (101) plane.

Based on the above descrived work, experimental results varied and a few reports are available on the detailled studies of the effect of solvents on zinc oxide properties. In addition, a variety of sol-gel approaches, which have started from the similar composition of a batch, provide a number of thin film materials which differ in properties [15, 22, 23]. So, the question of the influence of organic solvents used to prepare zinc oxide nanostructures still remains open.

In this paper, we prepare zinc oxide by spin-coating method using three different solvents such as 2-methoxyethanol, ethanol and isopropyl alcohol (IPA). These organic solvents have been selected regarding their relatively high dielectric constant and viscosity to dissolve the inorganic salts [22]. The morphological, structural, and chemical characteristics of the as-grown films were investigated in order to assess the crystal quality, orientation and purity. We perform characterization of as-grown films through X-ray diffraction analysis (XRD) and energy-dispersive X-ray spectroscopy (EDS) attached to the scanning electron microscopy (SEM) techniques to correlate the nature of solvents with the properties of the nanostructured films.

Experimental Procedure

Zinc acetate dihydrate ($Zn(CH_3COO)_2{\cdot}2H_2O$, 98% purity), Mono-ethanolamine (C_2H_7NO, 98% purity), from Merck Chemicals; 2-Methoxyethanol ($C_3H_8O_2$, 99% purity), ethanol (CH_3CHOH, Sigma-Aldrich, ACS reagent, 99%), and isopropyl alcohol ($(CH_3)_2CHOH$, Sigma-Aldrich, ACS reagent, 99%), acetone (CH_3COCH_3, Acros Organics, 99%) were purchased from Alfa Aesar Chemicals and used as received without any further purification.

For the preparation of films, zinc acetate dehydrate ($Zn(CH_3COO)_2{\cdot}2H_2O$) was used as the starting material. Organic solvents such as 2-methoxyethanol ($C_3H_8O_2$), ethanol (C_2H_6O) and isopropyl alcohol (C_3H_8O), and a stabilizer agent monoethanolamine ($H_2NC_2H_4OH$) (MEA) were used to prepare the precursor solution. 0.8 g zinc acetate dehydrate was first dissolved at room temperature in each solvent followed by the stabilizer. The molar ratio of MEA to zinc acetate dehydrate was kept at 1. Required concentration of all solutions was 0.75 M, and the resulting solutions were stirred at 60 °C during 2 hours to yield clear and homogeneous solutions which served as the coating solutions. Thus, three kinds of coating solutions with different solvents were prepared.

Prior to deposition, the glass substrates were ultrasonically cleaned with acetone, isopropanol and finally with deionized water for 15 min in each step and then dried using compressed air. The coating solutions were then spin coated on glass substrates at room temperature with a rate of 3000 rpm for 30s. After each layer deposition, the spin-coated ZnO/glass assembly was heat-treated at 300 °C for 10 min to evaporate the solvent and remove organic residual. The processing step was repeated for three times to obtain a desired thickness. Finally, the ZnO thin films were subsequently annealed at 550 °C for 2 h and characterized.

X-ray diffraction measurements were performed using XPERT-PRO X-ray diffractometer (CuKα radiation, λ = 1.54060 Å) operating at 35 kV and 30 mA. An angular range from 10 to 70° with a step size of 0.0670° was probed using a copper anode X-ray source. The theoretical peak positions for zinc oxide with their relative intensities were obtained from Inorganic Crystal Structure Database (ICSD). The microstructural parameters were also evaluated. The scanning electron microscopy (SEM) measurements on the samples were performed by JSM-6490 JEOL equipped with energy-dispersive X-ray spectroscopy (EDS) apparatus with a constant accelerating voltage of 20 kV.

Results and Discussion

Fig. 1(a-c) depicts the X-ray diffraction graphs of the sol-gel derived zinc oxide thin films prepared on glass substrates under three different solvents sources. Well-defned diffraction peaks corresponding to (002) and (101) planes are indexed. No peaks of any other phase were detected. The obtained XRD spectra matched well with the space group P63mc (186) (No. 36-1451) [29] for hexagonal zinc oxide with wurtzite structure. All the as-grown ZnO films exhibit the higher intensities of preferential orientation along (002) plane compared to other orientation as (101). In addition, the sharper diffraction peaks indicate that the as-synthetized films have good crystallinity [22, 23].

Two diffraction peaks corresponding to reflecting planes (002) and (101) appeared in Fig. 1(a, b), while in Fig.1c, one single peak (002) is observed. The high-intensity peak (002) is observed in ZnO films prepared with 2-methoxyethanol which indicates the quality growth along the (002) plane [23]. Liao (2013) [30] too observed the dominance of the (002) peak, as well as the enhancement of the c-axis orientation with 2-methoxyethanol.

The d-spacing values, structural parameters such as lattice constants ($a = b, c$) were obtained from the Bragg's law of the wurtzite structure and the theoretical equations from the XRD data using the following formulae [31] and tabulated in Table 1.

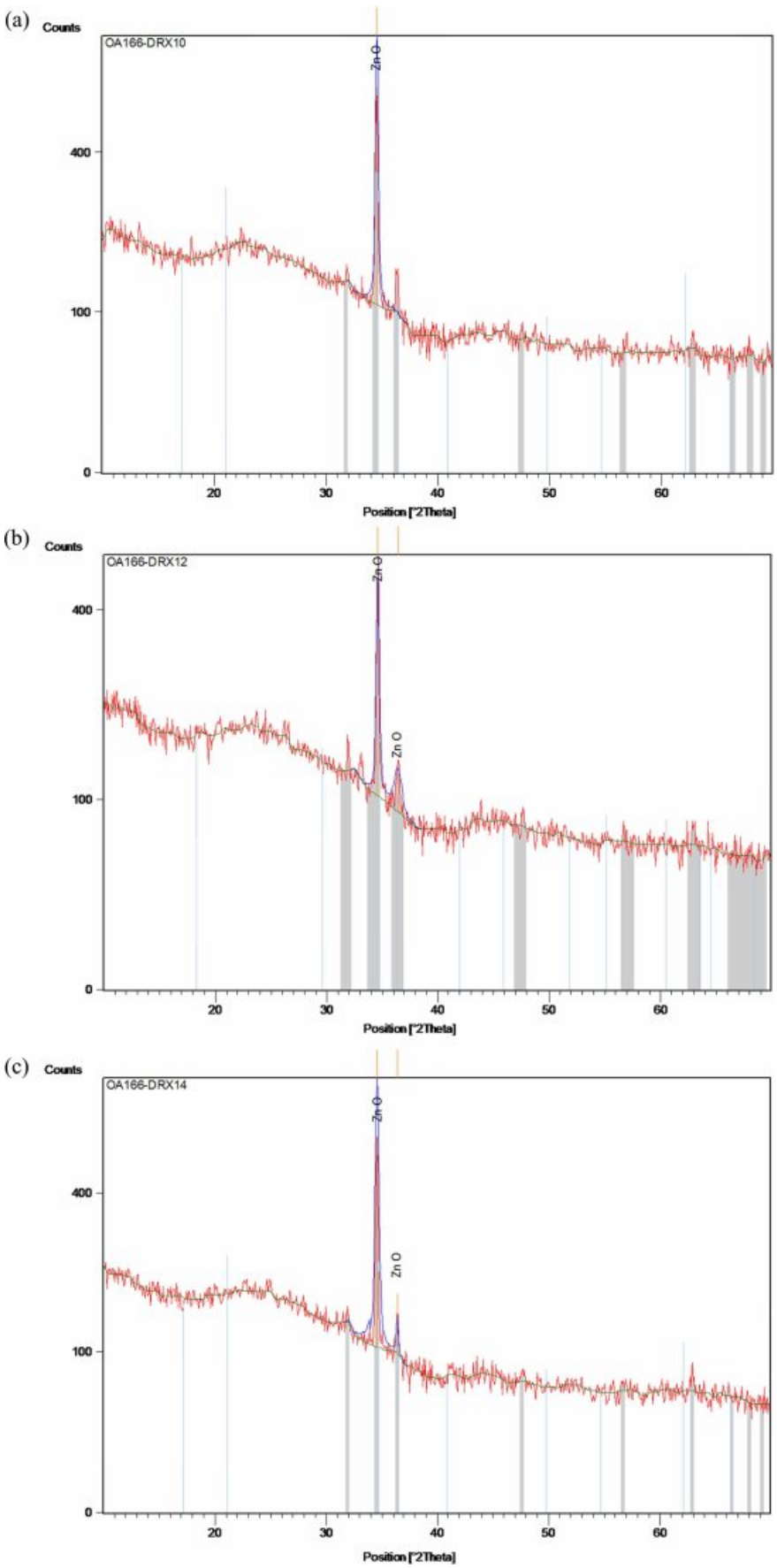

Fig. 1. DRX spectra of coated ZnO using (a) 2-methoxyethanol, (b) ethanol and (c) IPA.

$$\frac{1}{d_{hkl}^2} = \left(\frac{h^2 + hk + k^2}{a^2} \right) + \frac{l^2}{c^2} \quad (1)$$

$$a = \sqrt{\frac{1}{3}} \frac{\lambda}{\sin\theta_{hkl}} \quad (2)$$

$$c = \frac{\lambda}{\sin\theta_{hkl}} \quad (3)$$

The average crystallite sizes (D_{hkl}) of the nanostructures were computed according to broadening of the highest intensity peak corresponding to the (002) diffraction plane using Debye Scherer expression [32]:

$$D_{hkl} = \frac{0.9\lambda}{\beta\cos\theta_{hkl}} \quad (4)$$

Where λ is the X-ray wavelength of 1.54060Å, θ is the Bragg diffraction angle in degrees and β is the FWHM of (002) plane. The different average crystallite sizes for the samples are also listed in Table 1. As it can be seen the values are found in the nanometer region (1-100 nm), indicating that the polycrystalline zinc oxide films are made up of nanocrystal particles. The crystallite size values in the case of the coated films prepared with 2-methoxyethanol is bigger than those prepared with the other solvents.

For the bulk ZnO from the JCPDS data with card number 36-1451, the pure lattice constants 'a' and 'c' are 3.24982 and 5.20661 Å, respectively. Based on the results shown in Table 1, all of the ZnO thin films had lower lattice constant values compared with the bulk. The 'a' and 'c' values of the as-grown films with 2-methoxyethanol (a = 3.22181 Å and c = 5.20544 Å) were nearly closest to the bulk ZnO which indicate the good crystalline in nature [22]. Moreover, it can be seen that the interplanar spacing d_{hkl} decreases with the type of solvent.

Further information from the diffractograms can be obtained from an analysis of the texture coefficient, as defined by C. Barret et al. [33], as the preferred orientation, compared to the other observed orientations. The texture coefficient $TC_{(hkl)}$ of a plane (hkl) is calculated using the following relation [33].

$$TC_{(hkl)} = \frac{\frac{I(hkl)}{I_0(hkl)}}{\frac{1}{n}\sum_{i=1}^{n}\frac{I(hkl)}{I_0(hkl)}} \quad (5)$$

Where n is the number of diffraction peaks considered, I (hkl) is the measured relative intensity of the reflection from the (hkl) plane, and I_0 (hkl) represents the X-ray intensities from standard ZnO powder with randomly oriented grains [29]. Since, two reflection peaks were observed from (002) and (101) plane, for the extremely preferential orientation, T(hkl) = 2, while for the random one, T(hkl) = 1. The texture coefficients TC (002) and TC (101) of ZnO thin films are presented in Table 1. It can be seen that the three texture coefficients of the thin films vary avec the type solvent, and TC (002) with 2-methoxyethanol is near the extremely preferential orientation value. This result indicates that the thin films grown with 2-methoxyethanol exhibit the best c-axis-preferred orientation.

Scanning electron microscopy (SEM) morphologies of the as-grown thin films by different solvents are shown in Fig. 2(a-c).

The obtained SEM images show that all the ZnO thin films consist of spherical grains uniformly distributed throughout the surface and the slight changes in microstructure which can be attributed to the role of the solvents during the growth process of the films. ZnO crystalline grains with hexagonal morphology consistently appear on the substrate surfaces. The surface morphology also shows a high density of small grains and the crystalline quality is better improved with 2-methoxyethanol solvent because the grain size obviously becomes larger. The different degrees of brightness of the grains indicate the presence of multiple layers of ZnO on the substrates. The brighter grains represent the upper layer of the thin films and the darker grains represent the lower layer of the thin films. Surface morphology changes induced by these kinds of solvents were previously reported [23, 34].

EDS and elemental mapping analysis

EDS was used to check the elemental composition of

Table 1. Structural parameters variation with type of solvents

Sample	2-Theta (°)	Lattice parameters (Å)		d (002) (Å)	$D_{(002)}$ (nm)	Texture coefficient (002)
		a = b	c			
2-methoxyethanol	34.5078	3.22181	5.20544	2.59704	43	1.83
Ethanol	34.5592	3.21193	5.20362	2.59544	28	1.58
Isopropyl alcohol	34.5510	3.20917	5.20425	2.59389	34	1.65
JCPDS 36-1451	34.42	3.24982	5.20661	-	-	-

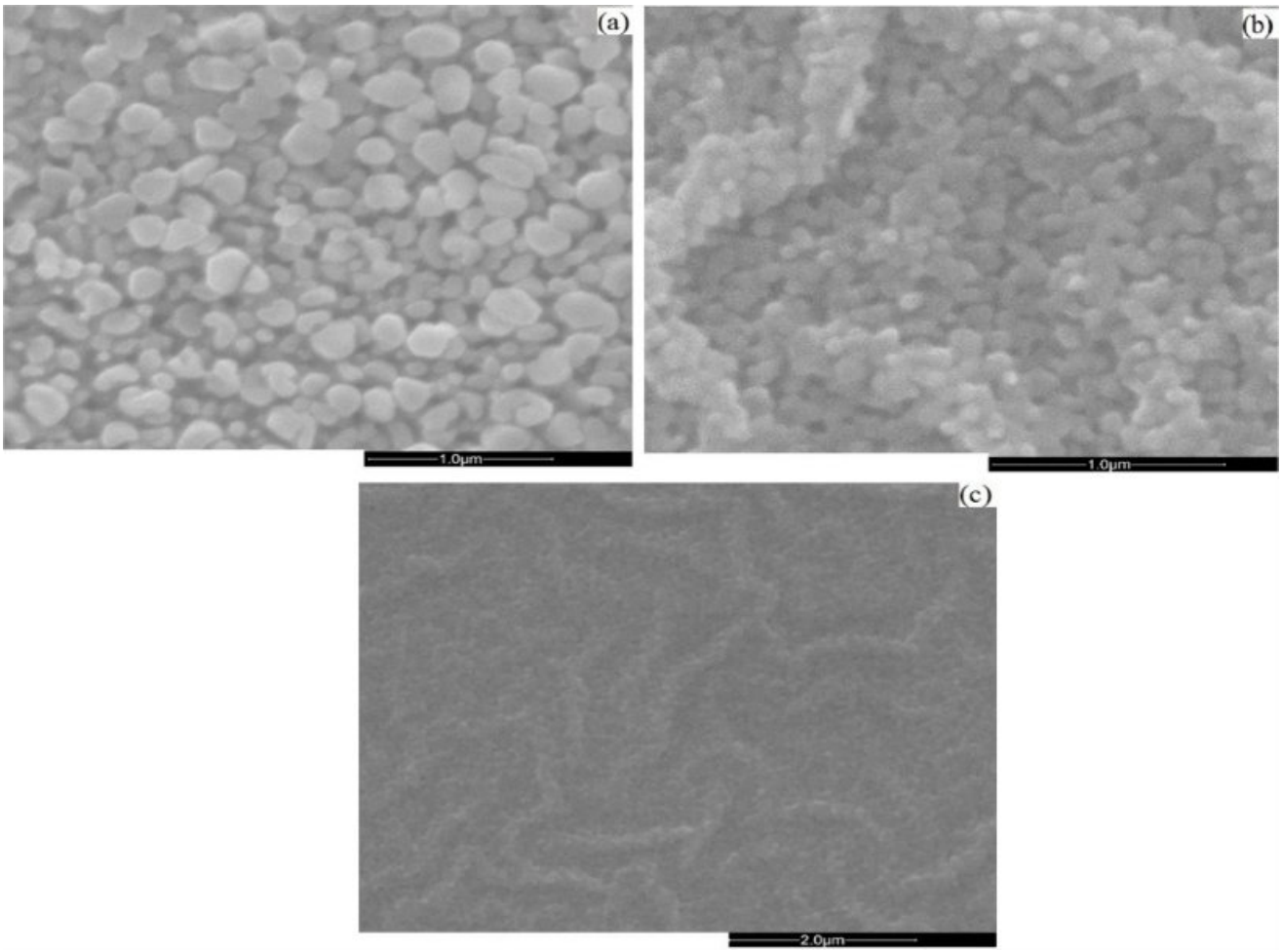

Fig. 2. SEM micrographs of as-grown ZnO films under conditions: (a) 2-methoxyethanol; (b) ethanol and (c) IPA

the coated thin films. The EDS pattern of the samples is shown in Fig. 3. The detected peaks indicated that, only zinc (Zn) and oxygen (O) were found in all the samples, their proportion varies under different solvents sources. A few peaks (Si, Ca, Mg) originated by the glass substrates were also detected.

The EDS analysis performed on ZnO (Fig. 3b) shows an excess of oxygen. This excess implies a non-stoichiometric Zn/O ratio. The compositional Zn map (Fig. 3a) confirms the homogenous distribution of Zn over the ZnO nanoparticles. In Fig. 3d and Fig. 3f, the EDS analysis of ZnO shows equally intense oxygen and zinc peaks with a slight excess of oxygen, leading to a non-stoichiometric Zn/O ratio.

Table 2. Chemical compositions of the ZnO nanoparticles

Sample	Zinc (at. %)	Oxygen (at. %)
2-methoxyethanol	41.3	58.7
Ethanol	48.6	51.4
Isopropyl alcohol	46.8	53.2

The acquired amounts of Zn and O were shown in Table 2. The existence of any other element was not recognized in the specimen, indicating the purity of the synthesized samples [23].

Conclusions

Chemical sol-gel via spin-coating method was successfully applied to synthesize zinc oxide thin thin films at room temperature using different solvents sources. XRD results show two peaks corresponding to the crystalline growth orientations of the (hkl) planes (002) and (101) depending on the type of solvents. All the synthesized films have hexagonal wurtzite structure oriented on the preferential plane (002). The average sizes ranged between 28-43 nm. SEM and EDS images revealed spherical particles with uniform size distribution with grains consisting of zinc and oxygen elements. The elemental mapping analysis revealed an excess of oxygen peak with 2-methoxyethanol samples and equally intense oxygen and zinc peaks with a slight excess of oxygen with ethanol and isopropyl alcohol samples.

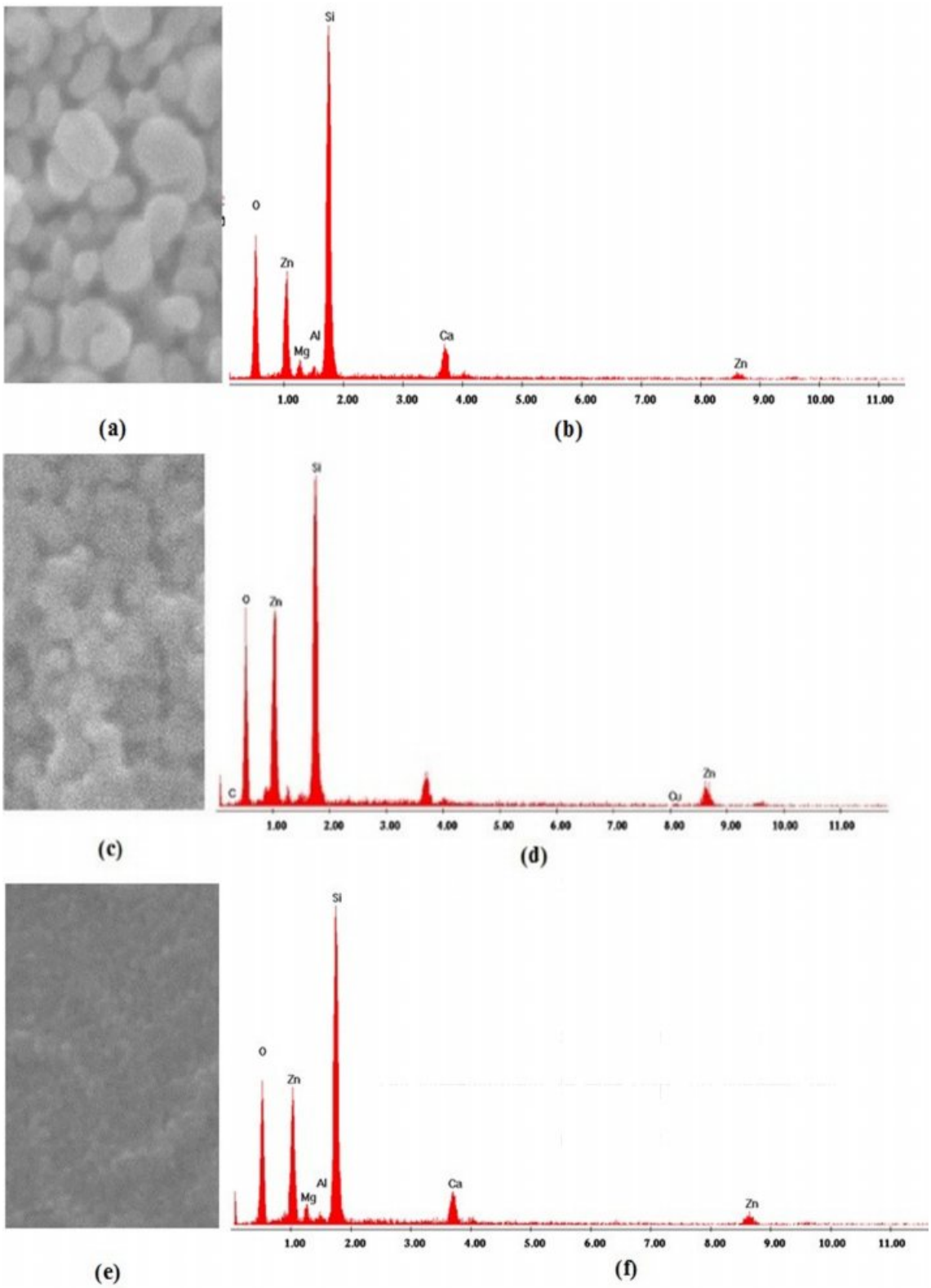

Fig. 3. EDS elemental Zn mapping (left) and spectra (right) in as-grown zinc oxide samples using 2-methoxyethanol, (b) ethanol and (c) IPA.

In summary, the type of solvents strongly affects the growth orientation (002) and the crystalline quality of the as-grown films. We can control zinc oxide preferential growth c-axis in wet chemical solution method by choosing the appropriate solvents. As 2-methoxyethanol, ethanol and IPA were used to prepare the ZnO films, the best solvent achieved for highly (002)-oriented zinc oxide thin film was 2-methoxyethanol.

Acknowledgements

The authors would like to pay sincere thanks to both University of Nanguy Abrogoua, Abidjan-Côte d'Ivoire and Hassan II University of Casablanca, Mohammedia, Morocco for the assistance.

References

1. M. Kim, J-M. Park, J-Y. Noh, J-I. Kim, M-J. Kang, and J-C. Pyun, Int. J. Nanotechnol. 15[6/7] (2018) 598-610.
2. C. Tsay, K. Fan, and C. Lei, J. Alloy. Compd. 512 (2012) 216-222.
3. M.A. Gondal, Z.H. Yamani, Q.A. Drmosh, and A. Rashid, Int. J. Nanoparticles 2[1/2/3/4/5/6] (2009) 119-128.
4. M. Caglar, S. Ilican, and Y. Caglar, Thin Solid Films 517 (2009) 5023-5028.
5. C.M. Muiva, T.S. Sathiaraj, and K. Maabong, Ceram. Int. 37 (2011) 555-560.
6. A. Ashour, M.A. Kaid, N.Z. El-Sayed, and A.A. Ibrahim, Appl. Surf. Sci. 252 (2006) 7844-7848.
7. Y. Zhang, Y-H. Wen, J-C. Zheng, and Z-Z. Zhu, Appl. Phys. Lett. 94, 113114 (2009); doi: 10.1063/1.3104852.
8. M., Wang, C.H. Ye, Y. Zhang, H.X. Wang, and L.D. Zhang, J. Mater. Sci.: Mater. Electron. 19 (2008) 211-216.
9. J.H. Lim, C.K. Kang, K.K. Kim, I.K. Park, D.K. Hwang, and S.J. Park, Adv. Mater. 18 (2006) 2720-2724.
10. Q, Wan, C.L. Lin, X.B. Yu, and T.H. Wang, Appl. Phys. Lett. 84 (2004) 124-126.
11. S.P. Usha, and B.D. Gupta, Appl. Optics, 56[20] (2017) https://doi.org/10.1364/AO.56.005716.
12. M.R. Khanlary, V. Vahedi, and A. Reyhani, Molecules 17 (2012) 5021-5029.
13. P. Zhan, Z. Li, and Z. Zhang, Mater. Trans. 52[9] (2011) 1764-1767.
14. K.M. Lee, C. W. Lai, K.S. Ngai, and J.C. Juan, Water Res. 88 (2016) 428-448.
15. Y. Guo, H. X. Zhu, Niu, W. Zhang, Z. Li, J. Chen, and Y. Mai, Advanced Engineering Materials, 18[8] (2016) 1418-1425.
16. C. C. Chena, N. Yea , C. F. Yu, and T. Fan, J. Ceram. Process. Res. 15[2] (2014) 102-106.
17. S. K. Hong, J. H. Lee, B. H. Cho, and W. B. Ko, J. Ceram. Process. Res. 12[2] (2011) 212-217.
18. O.A. Fouad, A.A. Ismail, Z.I. Zaki, and R.M. Mohamed, Appl. Catal. B-Environ. 62 (2006) 144-149.
19. G. Kaurn, A. Mitra, and K.L. Yadav, Progress in Natural Science: Materials International, 25 (2015) 12-21.
20. D.S. Kim, D. Lee, J.H. Lee, and D. Byun, J. Korean Phys. Soc. 64[10] (2014) 1524-1528.
21. Y.W. Heo, K. Ip, S.J. Pearton, D.P. Norton, and J.D. Budai, Applied Surface Science, 252 (2006) 7442-7448.
22. D. Sun, M. Wong, L. Sun, Y. Li, N. Miyatake, and H.J. Sue, J. Sol-Gel Sci. Technol., 43 (2007) 237-243.
23. F.K. Konan, J.S.N'cho, H.J. Tchognia Nkuissi, B. Hartiti, and B. Aka, Mater. Chem. Phys. 229 (2019) 330-333.
24. J. Wang, Y. Qi, Z. Zhi, J. Guo, M. Li, and Y. Zhang, Smart Mater. Struct. 16 (2007) 2673-2679.
25. P. Sagar, P.K. Shishodia, and R.M. Mehra, Appl. Surf. Sci. 253 (2007) 5419-5424.
26. S. Chakrabarti, D. Ganguli, and S. Chaudhuri, Mater. Lett. 58 (2004) 3952-3957.
27. L. Znaidi, G.J.A.A. Soler Illia, R. Le Guennic, and C. Sanchez, J. Sol-Gel Sci. Techn. 26 (2003) 817-821.
28. K.L. Foo, M. Kashif, U. Hashim, and W.-W. Liu, Ceram. Int. 40 (2014) 753-761.
29. Y.Y. Bu, and Y-M. Yeh, Ceram. Int. 38 (2012) 3869-3873.
30. Y. Liao, X. Zhou, X. Xie and Q. Yu. J. Mater. Sci: Mater Electron, 24 (2013) 4427-4432|.
31. F. H. Chung, Journal of Applied Crystallography 7 (1974) 519-525.
32. B.D. Cullity, and S.R. Stock, Element of X-ray Diffraction (Prentice-Hall, Inc.,), New Jersey (2001).
33. C. Barret, and T.B. Massalski, Structure of Metals, Pergamon Press, Oxford (1980) 204.
34. F.K. Konan, A. Beti, H.J. Tchognia Nkuissi, K. Dakshi, B. Aka, and B. Hartiti, J. Ceram. Process. Res. 18[12] (2017) 882-886.